Available online at www.sciencedirect.com
SCIENCE DIRECT
Journal of Power Sources 156 (2006) 692–699
JOURNAL OF POWER SOURCES
www.elsevier.com/locate/jpowsour

Investigation of the porosity of electrolytic manganese dioxide and its performance as alkaline cathode material

Deyang Qu *

Department of Chemistry, University of Massachusetts, Boston, MA 02125-3393, USA

Received 3 May 2005; received in revised form 6 June 2005; accepted 6 June 2005
Available online 18 August 2005

Abstract

The ionic diffusion rate and the electrochemically accessible surface area of the cathode, consisting of electrolytic manganese dioxide (EMD), were studied by means of ac impedance techniques. A simplified transmission line model was applied in the numerical fitting. The relationship between the pore size distribution and the ionic diffusion rate was investigated, as well as the pore size distribution and the cathode 'spring-back'. EMD with a considerable volume of large pores was found to be beneficial not only for the high-rate discharge, but also for the cathode process during cell manufacture.

Keywords: EMD; Porosity; Diffusion; 'Spring-back'; Impedance

1. Introduction

Small primary electrochemical cells have been commercially available for more than a century. The mostly commonly used primary cells are primary alkaline manganese dioxide/Zn cells, due to their unique performance characteristics and favorable cost structure. Recently, the growth of modern electronic devices, such as digital cameras, cell phones, MP3 players and high-tech toys requires batteries to be better suited for these high power applications. Despite significant advances in the development and commercialization of new battery systems, primary alkaline MnO_2/Zn cells still dominate the consumer battery market. Therefore, making the traditional alkaline cells more capable under high discharge rate conditions becomes extremely appealing. At the high-rate discharge conditions, only small portions of the active material is utilized. The discharge efficiency of an alkaline primary cell is limited by the ionic diffusion rate in the cathode, the proton diffusion rate in electrolytic manganese dioxide (EMD) and the pre-mature passivation of Zn anode. The relationship between the cathode porosity and the rate capability of an alkaline EMD cathode will be described in this paper. It will also explore the impact of the cathode porosity on the processability of the cathode material.

In the porous MnO_2 electrode, EMD particles are distributed in the matrix of highly conductive solid medium, consisting of graphite and the other additives. The particles of the fine powders stick together during the cathode formation processes. The inter-particle pores are formed in those aggregated particles. The pore size distribution of the inter-particle pores depends on the size and shape of the primary particles and how they are packed together. On the other hand, pores can also be formed within the primary particles. The characteristics of those pores are a result of the manufacturing processes of the material.

The mass transfer phenomenon plays a dominant role in the functioning of an EMD cathode. Two diffusion processes are involved in the discharge of a porous EMD cathode. One is the proton diffusion through the lattice of MnO_2, the other is the ionic diffusion in the matrix of the porous electrode. The proton diffusion process has been investigated by various authors [1–3]. The proton diffusion coefficient was measured by means of the ac impedance technique and more recently

* Tel.: +1 617 287 6035; fax: +1 617 287 6030.
E-mail address: Deyang.qu@umb.edu.

0378-7753/$ – see front matter © 2005 Published by Elsevier B.V.
doi:10.1016/j.jpowsour.2005.06.013

in the transmission line model by Qu [4,5]. At the medium- and low-rate discharge, the proton diffusion rate inside MnO_2 was considered as the rate-determining step, however, at the high-rate discharge, the ionic diffusion inside the matrix of the porous electrode cannot be neglected because the mass transfer may not be fast enough to support the electrochemical reaction. Lee et al. [6] investigated the correlation between the electrochemical performance of a MnO_2 cathode in a non-aqueous electrolyte with the electrode porosity and the pore size distribution. Even though the study was conducted on a thin electrode, in which the mass transfer was significantly faster than that in the thick cathode of bobbin design, Lee still found that both high porosity and a large percentage of macropore volume benefit the high-rate performance of Li/MnO_2 cells. Similar conclusions were reached by Qu and Shi [7] for the high surface area carbon electrode used in the super-capacitor applications. By means of ac impedance techniques and equivalent circuit fitting, the accessible time to the pores of different sizes was estimated. The relationship between the rate capability and the pore size distribution was discussed. Qu suggested that at the high-rate discharge, only the large pores of the electrode can be electrochemically accessed, while at low-rate discharge, most of the BET surface area can be utilized. In light of the study, the electrochemically accessible surface area for the porous EMD electrode was determined [4].

In addition to the studies relating the pore size distribution to the discharge rate capability of a porous electrode, Manev et al. [8] investigated the impact of formation pressure on the pore size distribution of a porous natural graphite anode for a Li-ion battery. Both the porosity and the mean pore radius of the electrode were found to be reduced at high impact pressure and during longer compacting time. Consequently, not only the specific capacity, but also the reproducibility of the graphite anode was reduced. Similar phenomena were reported by Qu [9] for the alkaline MnO_2 cathode. Qu suggested that the ionic diffusion rate in the large pores is faster than that in the small pores, thus, the cathode with the high percentage of large pores has better rate capability. In addition to the performance benefit, the porous electrode with the high percentage of large pores also demonstrated the process benefit by minimizing the 'spring-back' or 'rebounce' when the formation pressure was removed from the cathode. The detailed experimental evidence for the significance of the porosity for a porous MnO_2 electrode is reported.

2. Experimental details

2.1. Material

Three kinds of electrolytic manganese dioxide materials, manufactured with similar procedures but different pore size distribution profiles, were chosen for the investigation. EMDs with significantly different pore size distributions were chosen for the study of the pressure-related pore reformation. Those EMDs, however, may not be synthesized with similar processes. KS6 synthetic graphite was from Timcal. Teflon suspension (T-30) used was from DuPont.

2.2. Electrolyte, reference and counter electrodes

A 30 wt% aqueous potassium hydroxide solution was used as the electrolyte in all experiments at 298 ± 1 K. All potential reported were referred to Hg/HgO reference electrode immersed in KOH of the same concentration as the experimental electrolyte. A Ni-mesh counter electrode was used.

2.3. Construction of EMD electrode and electrochemical cell

The detailed description of the electrode construction and the design of the electrochemical cell were reported previously [4]. The MnO_2 electrode was made with EMD and KS6 graphite at 9:1 weight ratio. Additional 0.5 wt% T-30 (dry material) was added as binder. Two grams of the black mix was pressed to form a tablet 22.0 ± 0.2 mm in diameter and 1.8 ± 0.2 mm in thickness. A two-compartment cell was used. The EMD working electrode and the Ni counter electrode were housed in the separate cell compartments, which were linked by an electrolyte bridge. Spring pressure was applied to ensure good contact between the working electrode tablet and the Ni current collector. A Hg/HgO reference electrode was connected to the working electrode compartment by a luggin capillary. The electrode was vacuum wetted before discharge.

2.4. Determination of the surface area and the pore size distribution of EMD

For the pure EMD samples, the powders were degassed under vacuum at 110 °C overnight. N_2 was used as the absorption gas. The pore size distribution was determined using desorption isotherm by BJH method [10]. The surface area of the EMD was measured by means of a five-point BET method with N_2 as the absorption gas.

To investigate the impact of pressure, 0.5 g of the black mix (whose composition was described in Section 2.3) was pressed at 2 and 3 mT pressures, respectively, in a 0.31 in. diameter dye using a hand press. The resulting pellets were degassed overnight at 110 °C. The measurement procedures were the same as those used to measure the porosity of the EMD powders.

2.5. Experimental techniques and instrumental details

The ac impedance measurements were conducted by means of a Solartron Electrochemical Interface 1278 and a Solartron Frequency Response Analyzer 1285 controlled by ZPOLT and CORRWARE software. ZVIEW was used for the fitting of the ac impedance data. A Quantachrom NOVA-

1000 porosimeter was used for the determination of the BET surface area and the pore size distribution.

The EMD electrodes were discharged at two different rates—30.8 mA g^{-1} (C/10) and 61.6 mA g^{-1} (C/5).

3. Results and discussion

3.1. The kinetics of ionic diffusion inside the porous electrode

The model and equivalent circuit, which were reported previously [11], were used for the fitting of the ac impedance data. The porous MnO_2 electrode was represented by a transmission line equivalent circuit with Faraday resistance in the matrix. The equivalent circuit is shown in Fig. 1. The detailed mathematical treatments for the transmission line were reported by Levie [12]. The technique has been reported in many publications [13,14]. In a porous electrode, the various sized pores are distributed throughout the matrix of the whole electrode. The connections between the pores of various sizes create the network for the ionic diffusion. The ionic diffusion rate has a direct impact on the rate of electrochemical reaction. The discharge with high current density has to be supported by the fast ionic diffusion within the pores of the electrode matrix. Otherwise, the diffusion limit condition could soon be reached for a porous MnO_2 electrode. Then, the discharge overpotential will start to increase, shortening the service life of the battery. Less than half of the cathode's theoretical capacity (normally about 30–35%) in an AA alkaline cell can be utilized at 1 A discharge conditions, while significantly higher capacity can be released if discharged at the 100 mA rate.

Along with the other factors, the pore size distribution of a MnO_2 electrode has a significant impact on the ionic diffusion rate, since the pores with different sizes have different time constants. Thus, the ionic diffusion rate inside the pores of different sizes varies. When an ac signal is applied to a porous electrode, the signal penetration depth is comparable to the depth of the pores, a situation analogous to a RC transmission line network as shown in Fig. 1. The mathematical equation of the transmission line has the same form as the diffusion equation since the process taking place in an RC circuit may be treated as the electronic diffusion into a semi-infinite medium. Its impedance can be represented as:

$$Z = \sigma'\omega\left[\cos\left(\frac{1}{2}m\pi\right) - i\,\sin\left(\frac{1}{2}m\pi\right)\right], \quad 0 < m < 1$$

where σ' is the constant phase element (CPE) and m is the CPE exponent.

Theoretically, the number of RC elements in the general form of the transmission line model should be infinite in order to represent the complete picture of a porous electrode, since each RC element stands for $1/n$ part of the total surface area of the porous electrode and the surface area of the pores with various sizes has different time constant. Thus, n should approach infinity. To simplify the calculation, a five-RC elements model was used to investigate the porous MnO_2 electrode [11]. Each RC component represents on average 20% of the electrode surface area. It is reasonable to assume that the porous electrode is uniform, thus, the specific double layer capacitance (F cm^{-2}), Faradic resistance R_F and Warburg component σ, for a given cathode, are the same for each of the five RC elements. So, $R_1, R_2, \ldots, R_5$ can be regarded as the measurements of how difficult it is to electrochemically access the projected surface area or pores.

The rate capability of an electrode is directly related to the surface area of the electrode, since the current density (mA cm^{-2}) is inversely related to the electrode surface area. Under the same discharge current, the larger the surface area, the lower the local current density, thus, the lower the electrochemical overpotential. In the case of a flat electrode, the geometric surface area of the electrode is the electrochemically accessible surface area, but for a porous electrode, the surface area which can be used for the electrochemical reac-

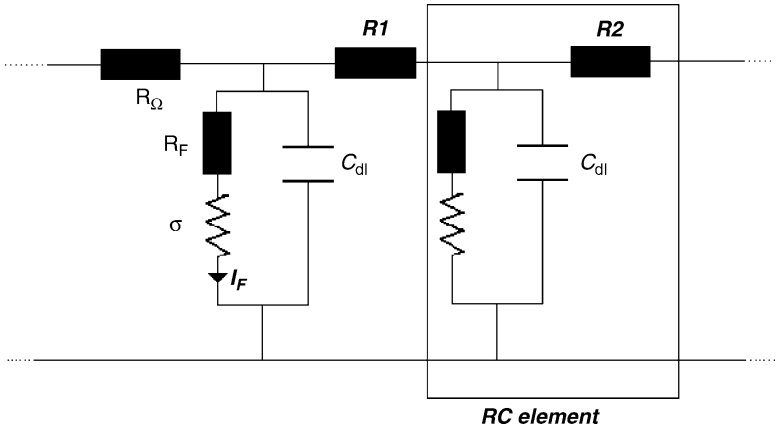

Fig. 1. Transmission line equivalent circuit used in the ac impedance fitting. Simplified circuit consists of five-RC components. R_Ω: ohmic resistance; R_F: Faradic resistance; C_{dl}: distributed double layer capacitance; σ: Warburg perfactor.

Table 1
Physical properties of the three EMDs

	EMD 1	EMD 2	EMD3
BET surface area ($m^2\ g^{-1}$)	34.96	31.78	45.20
Average pore size (Å)	24.45	36.34	20.90
Total pore volume ($cm^3 \times 10^{-2}$)	5.40	5.05	5.78
Pore volume for pore > 60 μm ($cm^3 \times 10^{-2}$)	1.8	1.5	0.84
Pore volume for pore < 15 μm ($cm^3 \times 10^{-2}$)	1.4	0.64	1.8
Mean particle size (μm)	54.03	52.62	48.24

tion is much smaller than the BET surface area, due to the fact that not all the pores in the porous electrode can be electrochemically accessed unless the electrode is discharged under very low current density. However, as soon as the surface area becomes accessed electrochemically, a double layer should be established.

In order to investigate the relationship between the pore size distribution of MnO_2 and the rate capability of the cathode, three EMD samples with different pore size distribution were chosen for the study. The properties of the EMDs are tabulated in Table 1. The pore size distribution for the three EMDs is shown in Fig. 2. It appears that the EMDs all consist of a sharp distribution of meso-pores with pore radius around 20 Å and a board distribution of large pores with pore radii between 60 and 400 Å. It is worth pointing out that the association of the 20 Å radius peak for EMD is still debatable, since the desorption isotherm may give anomalous results for MnO_2 around 19 Å radius because as pressure is lowered to the point where pores of 19 Å radius begin to desorb, the surface tension forces of the meniscus may be no longer strong enough to overcome the tendency for the liquid N_2 to boil and the smaller pores may empty almost at once, giving rise to a false peak. It has been observed that the shape and the height of the 19–20 Å radii peak was very sensitive to the degassing procedures. Although additional experimental work is needed to clarify the association of the peak, the conclusions of the paper regarding meso- and macropores are still valid, since the attentions were on the pores larger than 19 Å radius. The pores consist of both inter-particle pores and

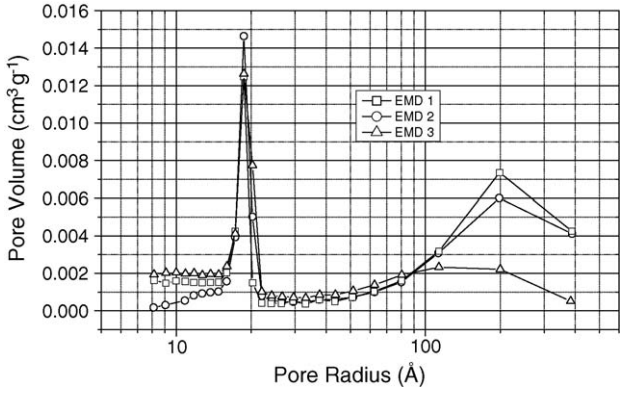

Fig. 2. Comparison of pore distribution of EMD 1–3 (calculated by BJH theory).

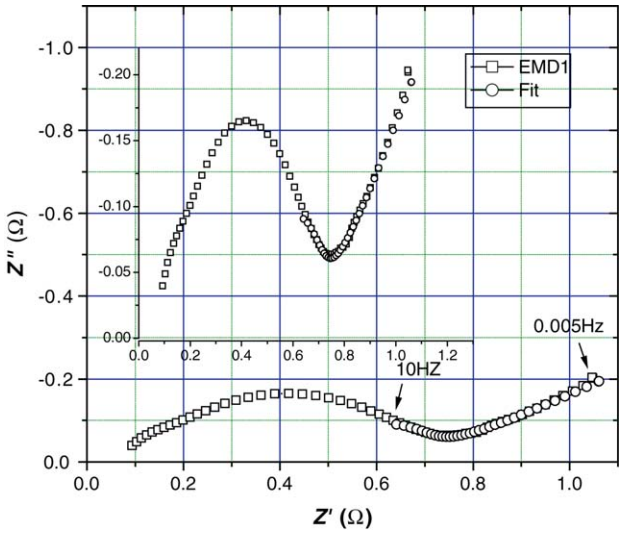

Fig. 3. The ac impedance response for non-discharged EMD electrode. Numerical fitting is based transmission line model shown in Fig. 1. The inset is the enlargement.

pores in the particles of EMD. Presumably, the larger pores are more likely to be the inter-particle pores. EMD1 has the highest large pore volume, while EMD3 has the largest BET surface area. The ac impedance was conducted on the cathodes made with the three EMDs. Fig. 3 shows the impedance spectrum with the fitting result obtained by using the transmission line model shown in Fig. 1. The figure inset shows the enlargement of the spectrum. It seems that the ac impedance can be well fitted using the model in the frequency range of 10–0.005 Hz. The medium to low frequency range was chosen to cover the broad range of pores, particularly, small pores. The fitting results are tabulated in Table 2. The Faradic resistance (R_F) and Warburg prefactor (σ) for all three EMDs are reasonably close to each other. It appears that the electrochemical characteristics, e.g. proton diffusion coefficient, are similar for the three EMD materials. So, it is reasonable to assume that all three EMDs have similar overpotentials resulting from the electrochemical processes related to the reduction of MnO_2.

Fig. 4 shows a comparison of the accumulated R for the three EMD cathodes. It appears that 25% of the most difficult accessible surface area has a large time constant and may not participate in the reduction reaction. The kinetics of the ionic diffusion in the pores which represent the bottom 25% of the surface area are very poor. According to Table 1, it seems that the most difficult accessible 25% of the sur-

Table 2
Fitting results based on equivalent circuit shown in Fig. 1

	EMD 1	EMD 2	EMD3
Ohmic resistance, R_Ω (Ω)	0.512	0.387	1.094
Charge transfer resistance, R_F (Ω)	0.045	0.036	0.042
Double layer capacitance, C_{dl} (F)	0.253	0.201	0.205
Warburg perfactor, σ	0.495	0.549	0.515

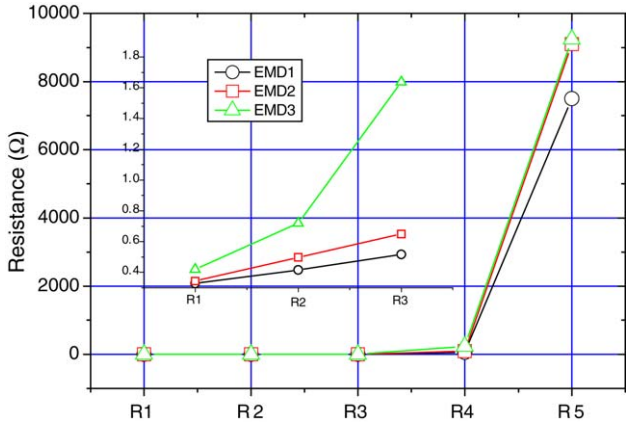

Fig. 4. Comparison of accumulated distributed resistance for the electrodes made with EMD1–3.

face area are for the pores with a size less than 15 Å. The inset in Fig. 4 shows the enlargement of the easiest accessible 50% of the surface area, which represents the most critical electrode/electrolyte interface for the electrochemical reaction at the high-rate discharge condition. It seems that among the three MnO_2 cathodes, the top 50% surface of the electrode made with EMD1 is the easiest to be electrochemically accessed, while that of the electrode made with EMD3 is the most difficult. Comparing the pore distribution profiles shown in Fig. 2, one may conclude that the surface area of the large pores can be easily accessed electrochemically. In other words, the ionic diffusion rate in the larger pores is faster than that in the smaller pores.

Fig. 5 shows the comparison of the discharge curves for the electrodes made with the three EMDs. Fig. 5A and B shows the discharge curves of 30.8 and 61.8 mA g^{-1}, respectively. It is obvious that there is little performance difference for the EMDs discharged at the low current density, but clear and significant difference can be observed for the electrodes discharged at the high current density as shown in Fig. 5B. EMD1, which has the largest volume of large pores, demonstrated the best high-rate performance, while EMD3, which has the lowest volume of large pores, has the poorest performance. Since all three EMDs were made using similar processes and have similar Faradic resistances and Warburg prefactors (Table 2), the electrochemical polarization and proton diffusion coefficients for all three EMDs should be close to each other. It is reasonable to assume that the major part of the performance difference resulted from the ionic diffusion process in the matrix of the porous electrodes. The discharge performances shown in Fig. 5 are in close agreement with the hypothesis, which predicts that the ionic diffusion rate is faster in the large pores, thus, the material with the large volume of big pores performs better at the high-rate discharge. Results shown in Figs. 2, 4 and 5 are in close agreement.

It is worth emphasizing that the critical parameter for the high-rate performance of a porous MnO_2 electrode is the pore

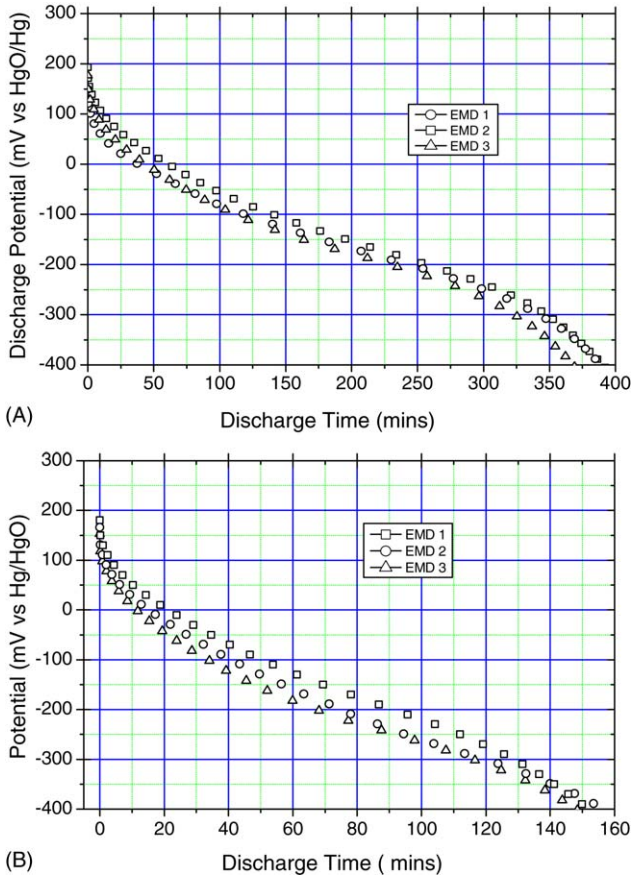

Fig. 5. Comparison of the discharge curves for cathodes made by EMD1–3 at 30.8 mA g^{-1} (A) and 61.6 mA g^{-1} (B).

volume of the large pores, not the total pore volume or the total porosity or the BET surface area. According to Table 1, EMD3 has the largest BET surface area and the largest pore volume; however, it was the worst high-rate performer among the three. The fact is that the high porous and high BET surface area material usually comprises a large number of small pores, which are more difficult to electrochemically access. In other words, the electrochemical utilization of the BET surface area is low for high porous material, owing to poor kinetics for the ionic diffusion in the small pores. Additionally, since the electrochemical studies were carried out in flooded cells with three-electrode configuration, the interactions between MnO_2 cathode and Zn anode in a cell were not considered, e.g. the electrolyte balance (generation and return of OH^- from cathode to anode), on which porosity may play a significant roles. The studies on full cells, in which all components being taking into consideration, are in progress and will be reported later.

3.2. The cause of electrode 'spring-back'

In the mass production of alkaline batteries, the EMD cathode was produced from the black mix of EMD and graphite by means of a dye press process. Hundreds of alkaline cells

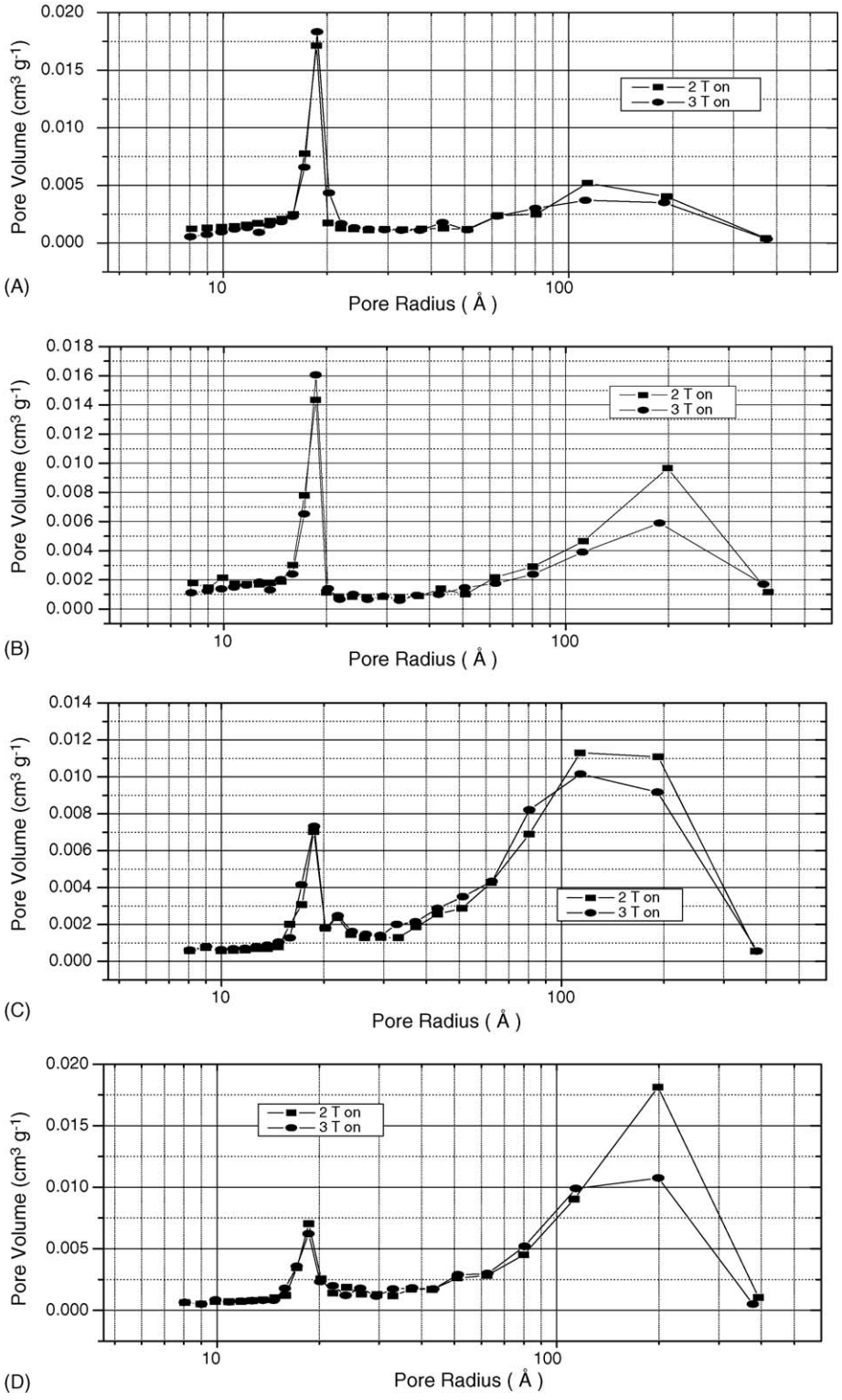

Fig. 6. Comparison of the changes of pore distribution for various EMDs after 2 and 3 mT compaction.

can be produced every minute on a modern high speed production line. So, the impact time for a single cathode ring is in the range of milliseconds. The spring-back is always a significant issue for the cathode process. The 'spring-back' or 'rebounce' is the phenomenon where after the formation pressure is removed and the cathode ring is ejected from the dye, the volume of the cathode ring expands and results in a decrease in the ring density. The cathode 'spring-back' ought

to be minimized due to the fact that large 'spring-back' will make the cathode ring move beyond the design dimension so that it cannot be inserted into the steel can. More importantly, large 'spring-back' will reduce not only the cathode density, but also the strength of the cathode tablet, which will result in low performance and high scrap rate. So, it is essential to understand the root cause for the cathode 'spring-back' and control it accordingly.

In a porous electrode, the particles of fine powders, called primary particles [12], will stick together due to the surface force and form secondary particles. The surface force only starts to take effect when the primary particles are forced close to each other by compression. Pores are formed in those aggregated particles. When the external compaction force is applied, the particles start to move, while the air trapped in the pores gets compressed. The force resulting from the compressed air will work against the particle movements. A portion of the trapped air will find its way out. Its space will be occupied by the solid particles and the porosity will be reduced. The air evacuation process is time dependent. So, the porosity reformation process during external compaction depends not only on the compaction pressure, but also on the dwell time. In the case of mass production, there is little room to adjust the dwell time, otherwise productivity will be affected. The trapped air remains compressed. When the dye pressure is removed from the cathode, the compressed air tends to expand and causes the cathode to 'spring-back'. So, in order to minimize the cathode expansion, the maximum amount of air should be removed from the matrix of the porous electrode.

The hypothesis was that the air trapped in the larger pores is much easier to remove than that in the smaller pores, since the large pores are easy to crack and will allow the solid particles to move in during the compaction. Fig. 6 shows the comparison of the change of the pore size distribution for four different EMD electrodes, after being compressed under 2 and 3 mT, respectively. It is clearly demonstrated that the high compaction force only reduces the pore volume of the large pores and the pore volume of the small pores is hardly changed. The pore reformation under external pressure is mainly done on the large pores. Fig. 7 shows the comparison of 'spring-back' for EMD1–3. The 'spring-back' was defined as the percentage of out-dye and in-dye volume change. Taking into consideration the pore size distributions for EMD 1–3 (Fig. 2), the relationship between the pore size distribution and 'spring-back' for the porous electrodes is clearly demonstrated. The cathode with the largest volume of large pores demonstrated least 'spring-back' and vice versa. It has to be noted that the 'spring-back' is the function of the cathode porosity, particularly, the inter-particle porosity. However, since the majority of the cathode is EMD, so the EMD porosity plays a dominant role in the cathode porosity.

Obviously, it is beneficial not only to the ionic diffusion within the matrix, but also to the processability of the porous electrode, to choose EMD with large volumes of

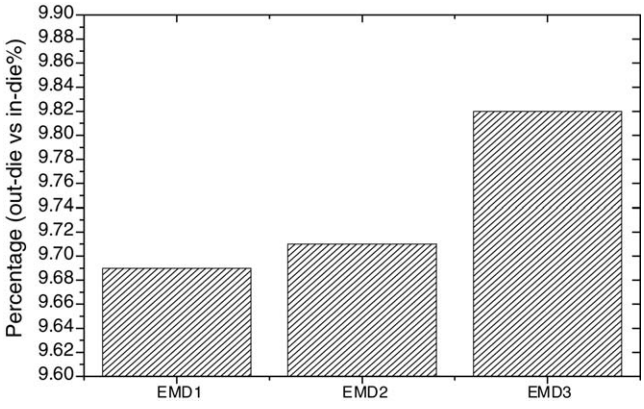

Fig. 7. Comparison of "spring-back" for EMD 1–3.

big pores. It should be emphasized that, on one hand, a strong and dense electrode with good contact conductivity should be made and on the other hand, the pressure should not be too high as to eliminate too many large pores which cause the ionic diffusion network to support the high-rate reduction of MnO_2. The compaction pressure should be optimized.

4. Conclusions

The significance of the pore size distribution of EMD has been investigated by means of ac impedance techniques, numerical fitting and 'spring-back' measurements. The following points are worth noting:

(1) The ionic diffusion rate inside the matrix of a porous electrode plays an important role in the rate discharge.
(2) The ionic diffusion rate inside the larger pores is faster than that in the smaller pores.
(3) EMD with a large volume of big pores performs better at the high-rate discharge.
(4) The ionic diffusion rate inside the porous electrode can be estimated by means of a transmission line model.
(5) Under compaction pressure, large pores are easily filled by the fine particles.
(6) 'Spring-back' results from the expansion of the compressed air trapped inside the small pores.
(7) EMD with large volumes of large pores has less 'spring-back'.

References

[1] S. Atlung, T. Jacobsen, Electrochim. Acta 21 (1976) 575.
[2] H. Zheng, X. Xia, J. Electrochem. Soc. 136 (1989) 2771.
[3] Y. Chabre, J. Pannetier, Prog. Solid State Chem. 23 (1995) 1.
[4] D. Qu, Electrochim. Acta 48 (2003) 1675.
[5] D. Qu, Electrochim. Acta 49 (2004) 657.
[6] T.J. Lee, T.T. Cheng, H.K. Juang, S.Y. Chen, J. Power Sources 44 (1993) 709.

[7] D. Qu, H. Shi, J. Power Sources 74 (1998) 99.
[8] V. Manev, I. Naidenov, B. Puresheva, G. Pistoia, J. Power Sources 57 (1995) 133.
[9] D. Qu, US 2003/0049531 A1.
[10] S.J. Gregg, K.S.W. Sing, Adsorption, Surface Area and Porosity, Academic Press, London, 1982.
[11] D. Qu, J. Power Sources 102 (2001) 270.
[12] R. De Levie, Electrochim. Acta 8 (1963) 751.
[13] J.-P. Candy, P. Fouilloux, M. Keddam, H. Takenouti, Electrochim. Acta 26 (1981) 1029.
[14] R.D. Armstrong, D. Eyre, W.P. Race, A. Ince, J. Appl. Electrochem. 1 (1971) 179.